JEM

SUPPLEMENTAL MATERIAL

Föger et al., http://www.jem.org/cgi/content/full/jem.20101757/DC1

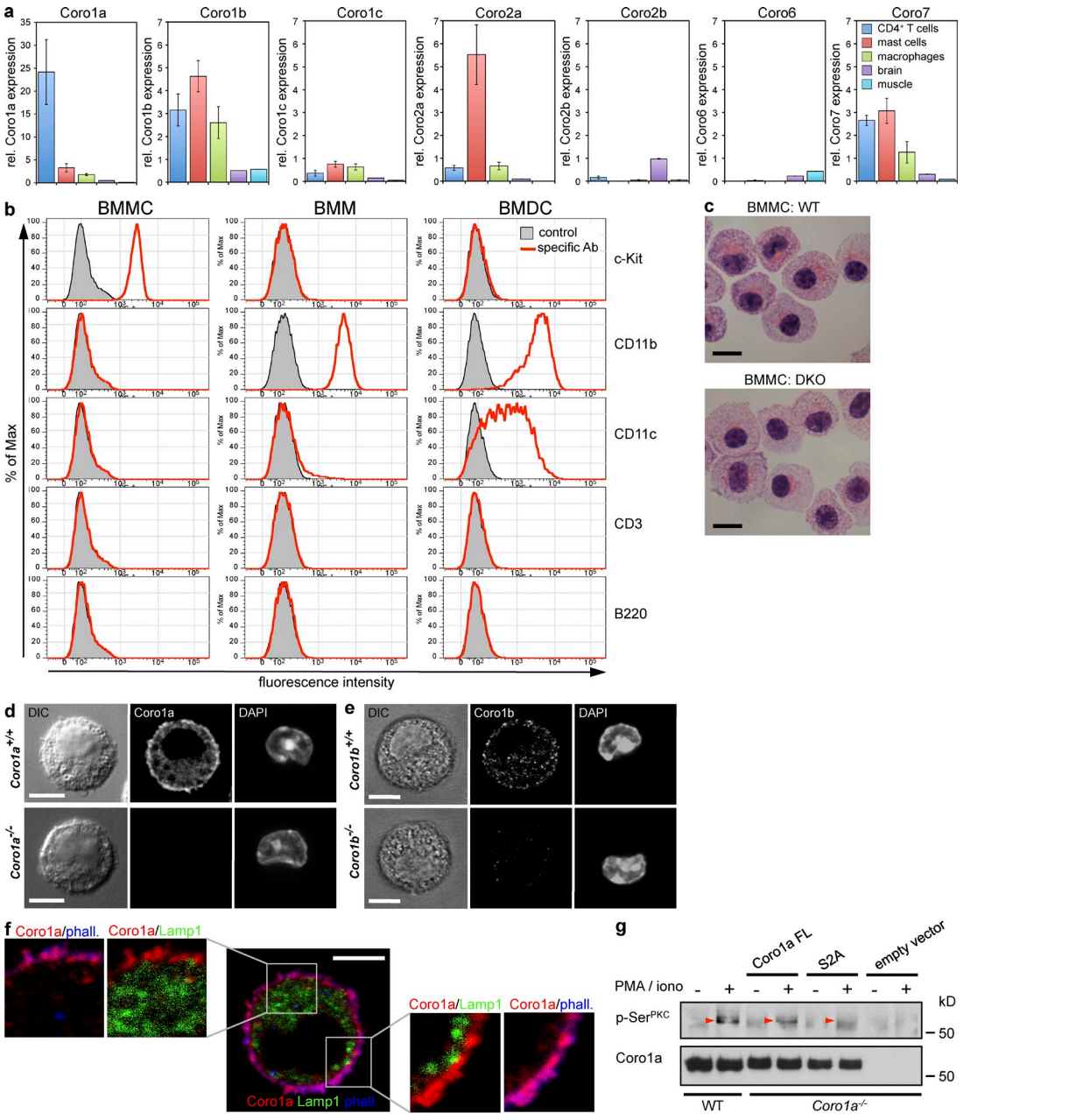

Figure S1. Expression of coronin family members in different tissues and cell types. (a) Quantitative real-time PCR analysis of mRNA expression of coronin family members in purified mouse primary CD4+ T cells, BMMCs, or BM-derived macrophages and brain and muscle tissue. Data are relative to HPRT and show the mean ± SD from two to three independent experiments with duplicate samples each. (b) Flow cytometric analysis of cell surface marker expression (c-Kit, CD11b, CD11c, CD3, and B220) on BMMCs, BM-derived macrophages, and BM-derived DCs. Red histograms represent the expression of the indicated cell surface marker, whereas the gray-filled histograms show the staining with isotype-matched control antibodies. Data are representative for two independent experiments. (c) Cytospins from WT or *Coro1*$^{-/-}$*Coro1b*$^{-/-}$ (DKO) BMMCs were subjected to Giemsa staining. Photos were taken with a light microscope (DM LB2 equipped with PL FLUOTAR optics; Leica). (d and e) Confocal microscopy analysis of *Coro1a*$^{+/+}$ and *Coro1a*$^{-/-}$ (d) or *Coro1b*$^{+/+}$ and *Coro1b*$^{-/-}$ BMMCs (e) stained for Coro1a (d) or Coro1b (e), together with DAPI, demonstrating the specificity of the coronin stainings. (f) Immunofluorescence staining of BMMCs stained for Coro1a, CD107a (Lamp1), and F-actin (phalloidin). Individual and overlay fluorescence images and magnifications were generated by confocal microscopy and are representative for at least three independent experiments. (g) Activation-induced Ser phosphorylation of the Coro1a-S2A mutant (S2A) is reduced compared with the WT full-length coronin protein (Coro1a FL). WT or *Coro1a*$^{-/-}$ BMMCs transiently transfected with the indicated expression constructs were stimulated with PMA/ionomycin or left untreated. Coro1a was immunoprecipitated from cellular lysates and immunoblotted with anti–p-Ser^{PKC} and anti-Coro1a to monitor Coro1a Ser phosphorylation. Ser-phosphorylated Coro1a is indicated by the red arrowheads. Similar results were observed in three independent experiments. Bars: (c) 10 µm; (d–f) 5 µm.

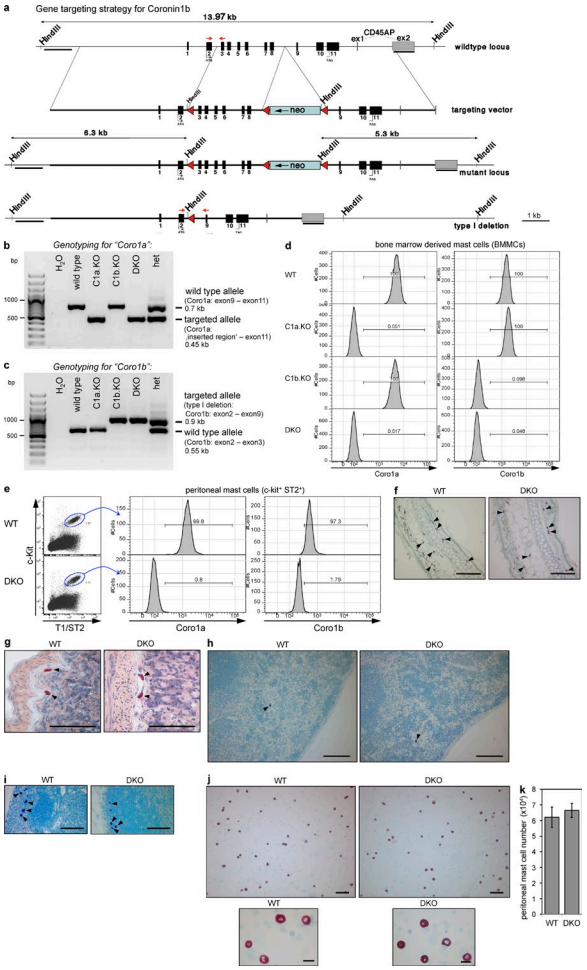

Figure S2. Generation of *Coro1b*$^{-/-}$ mice and histological analysis of MCs in *Coro1a*$^{-/-}$*Coro1b*$^{-/-}$ mice. (a) Gene targeting strategy. Endogenous (WT) Coro1b locus, targeting vector (middle), and targeted (mutant) Coro1b locus after homologous recombination. Total Cre-mediated excision of the region within the two outer loxP sites (red triangles) results in deletion of exons 3–8 (type I deletion). The targeting construct was electroporated into 129 RW4 embryonic stem cells. Targeted embryonic stem cell clones were identified by Southern blotting and microinjected into C57BL/6 blastocysts, and the resulting male chimeras were crossed with female C57BL/6 mice. Germline transmission was confirmed by polymerase chain reaction and Southern blot analysis of genomic tail DNA. These floxed-targeted lines were crossed with the EIIaCre transgenic mouse line to obtain Cre-mediated total germline excision of the loxP-flanked DNA sequences (type I deletion). Deletion was confirmed on the level of DNA, RNA, and protein. (b) PCR genotyping for Coro1a. Genomic DNA from WT, *Coro1a*$^{-/-}$ (C1a.KO), *Coro1b*$^{-/-}$ (C1b.KO), and *Coro1a*$^{-/-}$*Coro1b*$^{-/-}$ (DKO) mice and a heterozygous control were subjected to PCR analysis using primers specifically recognizing the WT allele (exon 9–11) and the targeted allele (inserted region – exon11). Primer used sequences were as follows: exon9 sense, 5′-CTTCATGAGCGGAAGTGTGA-3′; exon 11 antisense, 5′-CGCTCTTGTAGCTTTTGCAC-3′; and primer specific for the inserted region, 5′-CCAAGCCTATGCCTACAGC-3′. The size of the expected PCR products is indicated. (c) PCR genotyping for Coro1b. Genomic DNA from the indicated mice was subjected to PCR analysis using primers specifically recognizing the WT allele (exon 2–3) and the targeted allele (exon 2–9). Primer sequences used were as follows: exon 2 sense, 5′-CAGAGCAAATTCCGGCATGT-3′; exon 3 antisense, 5′-GACTTCATCATTGTGGGGAC-3′; and exon 9 antisense, 5′-CTCACACTTGCGTTCATGCA-3′. The size of the expected PCR products is indicated. Dozens of independent experiments were performed for b and c. (d and e) Expression of Coro1a and Coro1b in BMMCs (d) and peritoneal MCs (c-Kit^{+}T1/ST2^{+}; e). Cells of the indicated genotype were fixed, permeabilized, and subjected to intracellular staining with antibodies specific for Coro1a or Coro1b. In e, cells had also been subjected to cell surface staining for c-Kit and T1/ST2 to identify peritoneal MCs (c-Kit^{+}T1/ST2^{+} cells; gating is shown in the left panel). Numbers indicate the percentage of positive cells. Data are representative for two independent experiments. (f–i) Histological analysis of MCs in ear (f), stomach (g), spleen (h), and lymph node (i) of WT and *Coro1*$^{-/-}$*Coro1b*$^{-/-}$ (DKO) mice. Tissue sections were subjected to toluidine blue staining (f, h, and i) or naphtolesterase staining counterstained with hematoxylin (g). Arrowheads indicate MCs. (j) Cytospins of cells form peritoneal lavage from WT and *Coro1*$^{-/-}$*Coro1b*$^{-/-}$ (DKO) mice were subjected to toluidine blue staining and counterstaining with hematoxylin. Overview in the top panel demonstrates comparable frequency of peritoneal MCs in WT and DKO mice. The bottom panel shows normal morphology of *Coro1*$^{-/-}$*Coro1b*$^{-/-}$ peritoneal MCs. Histology was performed as described in Orinska et al. (2010), and photos were taken with a light microscope (DM LB2 equipped with PL FLUOTAR optics; Leica). (k) Absolute numbers of c-Kit^{+}T1/ST2^{+} peritoneal MCs of WT and *Coro1*$^{-/-}$*Coro1b*$^{-/-}$ (DKO) mice. Peritoneal lavage cells were analyzed by flow cytometry for the percentage of c-Kit and T1/ST2 double-positive cells, and the number of peritoneal MCs (c-Kit^{+}T1/ST2^{+}) was then calculated from the total number of peritoneal cells. Data are pooled from four independent experiments and show mean values ± SD (n = 9). Bars: (f–i and j [top]) 100 µm; (j, bottom) 20 µm.

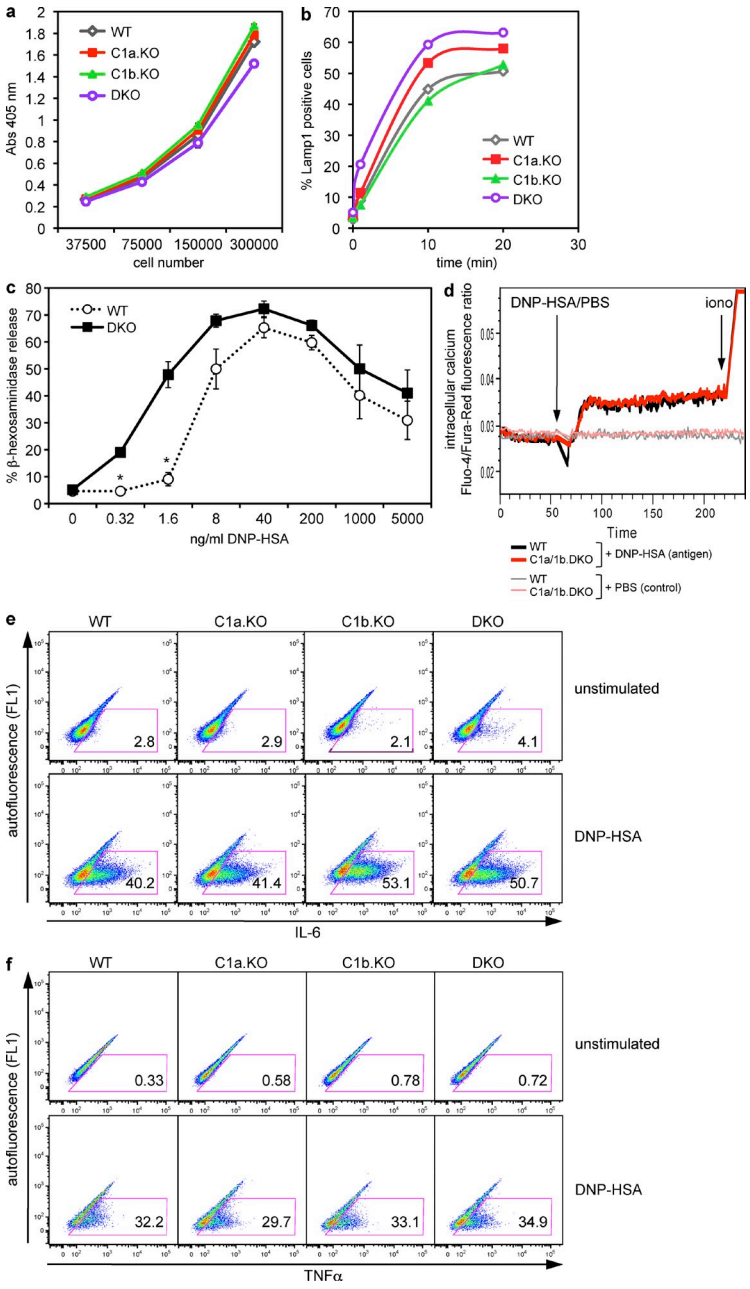

Figure S3. FcεRI-mediated degranulation, calcium mobilization, and intracellular cytokine production of *Coro1a*$^{-/-}$*Coro1b*$^{-/-}$ BMMCs. (a) Total cellular β-hexosaminidase was determined in lysates from serial dilutions of WT, *Coro1a*$^{-/-}$ (C1a.KO), *Coro1b*$^{-/-}$ (C1b.KO), and *Coro1a*$^{-/-}$*Coro1b*$^{-/-}$ (DKO) BMMCs as described in Materials and methods. Data are representative of three independent experiments. (b) Time kinetics of FcεRI-induced MC degranulation. Sensitized BMMCs were stimulated with 30 ng/ml DNP-HSA at 37°C for the indicated times, and degranulation was analyzed by determining CD107 (Lamp1) surface expression. Data show the percentage of CD107a-positive cells and are representative of two independent experiments. (c) FcεRI-induced β-hexosaminidase release. Indicated BMMCs were sensitized with anti-DNP IgE and stimulated for 10 min with the indicated concentrations of DNP-HSA. Data are means ± SD of duplicate cultures and representative of two independent experiments (*, $P < 0.01$). (d) FcεRI-induced calcium influx. Sensitized WT and *Coro1a*$^{-/-}$*Coro1b*$^{-/-}$ BMMCs were dual loaded with the fluorescent calcium indicators Fluo-4 and Fura-red as described by Parravicini et al. (2002). Baseline fluorescence readings were recorded by flow cytometry and then DNP-HSA was added at a final concentration of 10 ng/ml to induce calcium mobilization. Ionomycin was added at the end of the measurement to achieve maximal calcium flux. PBS was used as a negative control. Calcium mobilization is expressed as the ratio of Fluo-4 and Fura-red fluorescence intensity over time. Data are representative for three independent experiments. (e and f) Intracellular cytokine production. Sensitized BMMCs were stimulated for 4 h with 10 ng/ml DNP-HSA in the presence of Brefeldin A. Cells were analyzed for intracellular IL-6 (e) or TNF expression (f) by flow cytometry. Numbers indicate the percentage of positive cells. Data are representative for two independent experiments.

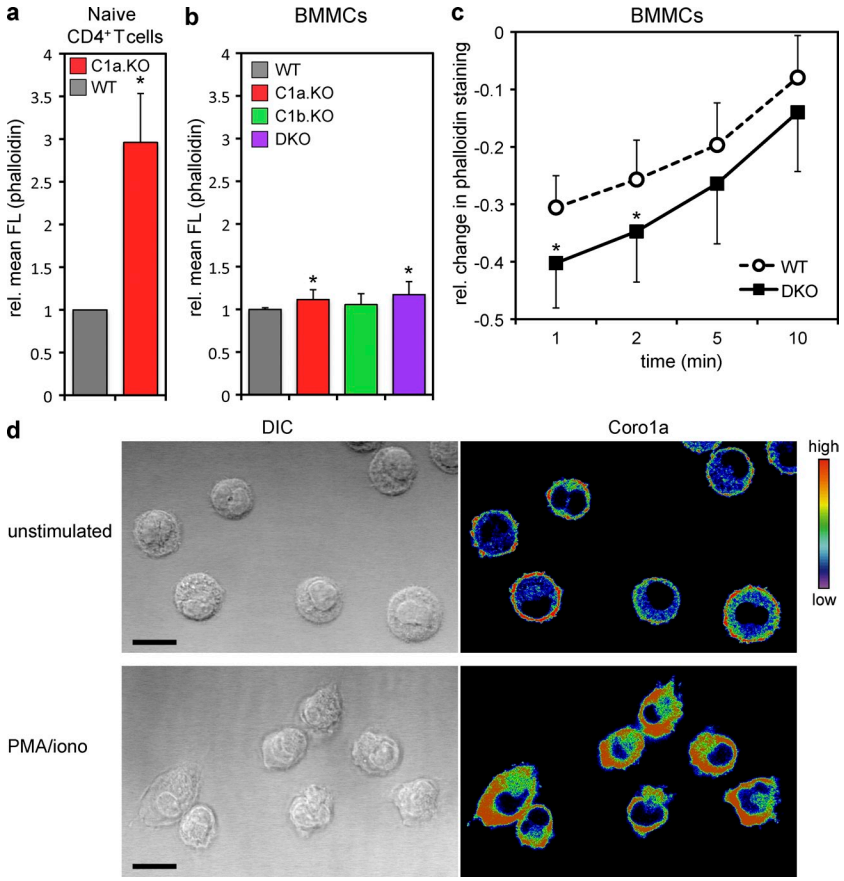

Figure S4. F-actin contents and cytoskeletal dynamics in BMMCs. (a and b) Cellular F-actin contents in naive ($CD44^{low}$) $CD4^+$ T cells (a) and BMMCs (b). WT, *Coro1a*$^{-/-}$ (C1a.KO), *Coro1b*$^{-/-}$ (C1b.KO), and *Coro1a*$^{-/-}$*Coro1b*$^{-/-}$ (DKO) cells were fixed, permeabilized, and stained with fluorescent-labeled phalloidin. Cells were analyzed for phalloidin staining by flow cytometry, and the relative mean fluorescence intensity was determined (the mean fluorescence intensity of WT cells was set to 1). *, $P < 0.001$. Graphs show cumulative mean data ± SD ($n = 6$ for naive T cells and $n = 21$ for BMMCs) from 4 (a) and 12 (b) independent experiments. (c) Relative changes in cellular F-actin levels upon FcεRI-induced MC activation. Sensitized WT and *Coro1a*$^{-/-}$*Coro1b*$^{-/-}$ (DKO) BMMCs were stimulated with 10 ng/ml DNP-HSA at 37°C for 1, 2, 5, and 10 min. Cells were then fixed, permeabilized, stained with fluorescent-labeled phalloidin, and analyzed by flow cytometry to determine the relative mean fluorescence intensity (the mean fluorescence intensity of WT cells was normalized to 1). Data show the relative change in phalloidin staining compared with unstimulated cells and are cumulative mean data ± SEM from 12 independent experiments. *, $P < 0.05$ (Wilcoxon matched pairs test). (d) Confocal microscopy images showing the subcellular redistribution of Coro1a upon MC activation. BMMCs were either left untreated or were stimulated with PMA/ionomycin for 10 min at 37°C. Cells were fixed, permeabilized, and subjected to immunofluorescence staining for Coro1a. Representative images from two independent experiments are shown. Bars, 5 µm.

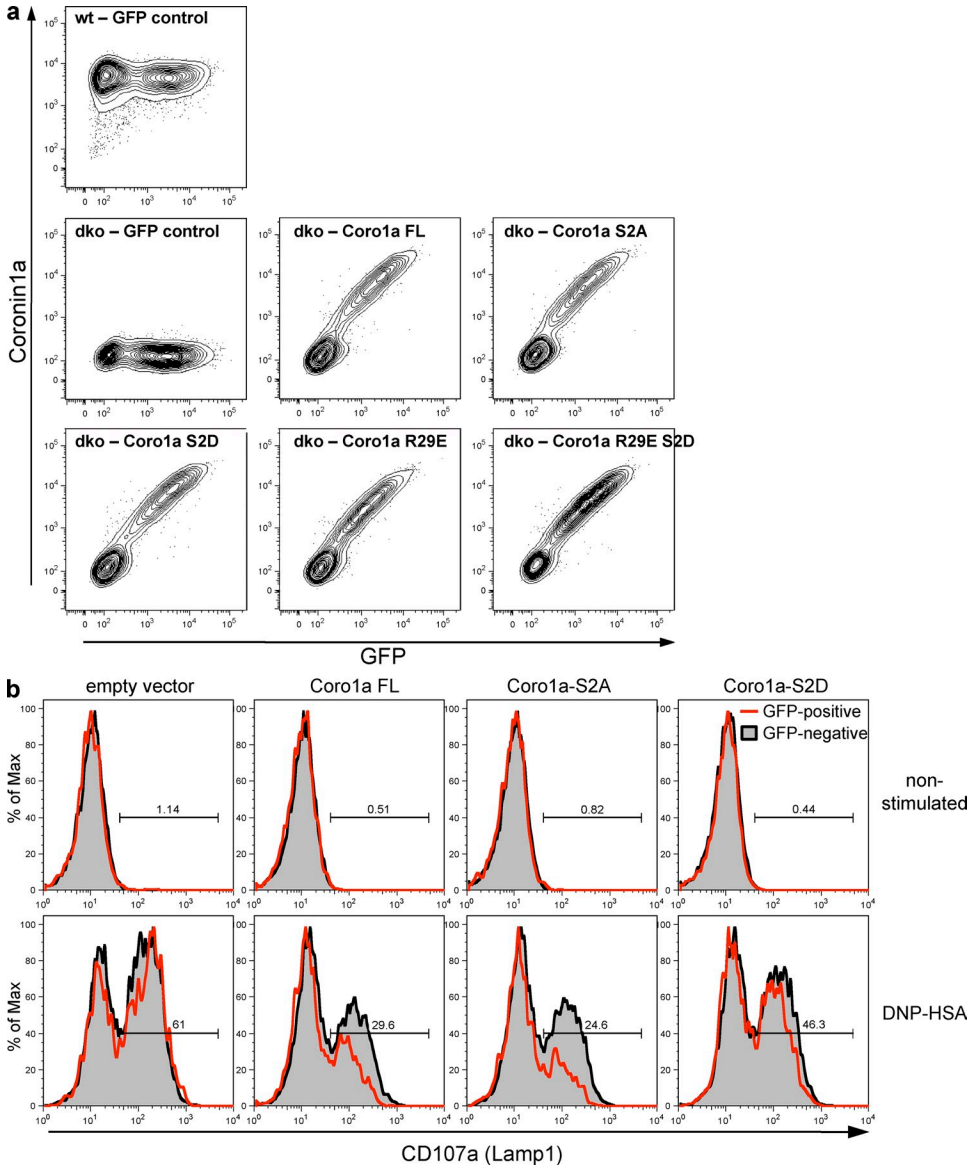

Figure S5. Transfection and functional reconstitution of *Coro1a*$^{-/-}$*Coro1b*$^{-/-}$ BMMCs. (a) Expression levels of coronin constructs in WT or *Coro1a*$^{-/-}$*Coro1b*$^{-/-}$ (dko) BMMCs transiently transfected with the indicated Coro1a–internal ribosomal entry site–GFP expression constructs or the empty vector (GFP control). Flow cytometric dot blots show intracellular staining for Coro1a and GFP. Data are representative for at least two independent experiments. (b) Functional reconstitution of MC degranulation. *Coro1a*$^{-/-}$*Coro1b*$^{-/-}$ BMMCs were transfected with Flag-tagged WT (Coro1a FL) or mutant Coro1a–internal ribosomal entry site–GFP expression constructs. Cells were sensitized with anti-DNP IgE and stimulated for 10 min with 10 ng/ml DNP-HSA. MC degranulation was assessed by analysis of CD107a (Lamp1) cell surface expression. Flow cytometric histogram shows overlays of CD107a surface expression on transfected (GFP positive) cells (red line) and nontransfected (GFP negative) cells (gray filled). Dead cells were excluded by propidium iodide staining. Numbers in the histograms indicate the percentage of CD107a-positive cells within transfected cells. Results are representative of four independent experiments.

Table S1. Primer combinations and the corresponding TaqMan probes utilized for quantitative real-time PCR

Gene	Left primer	Right primer	Universal ProbeLibrary (probe ID)
HPRT	5′-TCCTCCTCAGACCGCTTTT-3′	5′-CCTGGTTCATCATCGCTAATC-3′	#95
TNF	5′-CTGTAGCCCACGTCGTAGC-3′	5′-TTGAGATCCATGCCGTTG-3′	#78
IL-6	5′-TCTAATTCATATCTTCAACCAAGAGG-3′	5′-TGGTCCTTAGCCACTCCTTC-3′	#78
IL-13	5′-CCTCTGACCCTTAAGGAGCTTAT-3′	5′-CGTTGCACAGGGGAGTCT-3′	#17
Coro1a	5′-CTACTTGGGAGGGGTCACG-3′	5′-TTTGCTGGAGCGAACCAC-3′	#18
Coro1b	5′-TTCAGCCGCATGAGTGAAC-3′	5′-GTAGAGCCCCATTGCTTGAA-3′	#17
Coro1c	5′-ACCCCAGGAAACAGGAGATT-3′	5′-AGCCAGTAGTGAAGACGTTGC-3′	#72
Coro2a	5′-CCTTCTTTGACTCGGACACC-3′	5′-GTAGCGGATGTTCCCGTCT-3′	#60
Coro2b	5′-CCCACCCAGGACAGAGAAT-3′	5′-TGTCCTTCTGTGCCAGCTC-3′	#18
Coro6	5′-AGGTGGAGGTGCCTTCATT-3′	5′-CCAGTGACCAGTGGGTAGTTC-3′	#34
Coro7	5′-ATCACCTGACCCTCACAAGG-3′	5′-TCCACATCCTGAATGTCACAC-3′	#29

TaqMan probes (Universal ProbeLibrary ID numbers) were obtained from Roche.

Table S2. Quantification of colocalization

Staining markers	Pearson's coefficient
Coro1a/phalloidin	0.844 ± 0.060
Coro1a/CD107a (Lamp1)	0.291 ± 0.056
Coro1a/DAPI	0.002 ± 0.020
Coro1b/phalloidin	0.354 ± 0.108
Coro1b/CD107a (Lamp1)	0.316 ± 0.080
Coro1b/DAPI	0.007 ± 0.036

The level of colocalization between Coro1a or Coro1b and phalloidin, CD107a (Lamp1), or DAPI staining in confocal pictures of BMMCs was analyzed by determining the Pearson's correlation coefficient using iVisionEvaluation software. Values represent cumulative mean data ± SD (Coro1a, $n = 6$; Coro1b, $n = 5$).

Table S3. Quantification of immunoblots shown in Fig. 1 a

Sample	Coro1a/actin	Coro1b/actin
Thymus	2.84	0.43
Lymph node	1.68	0.75
Spleen	1.78	0.46
MCs	0.78	1.07
Macrophages	0.15	0.19
DCs	0.51	0.57

Densitometric quantification of the immunoblots shown in Fig. 1 a was performed using ImageJ software. The actin loading control was utilized to normalize values. Values are reported in arbitrary units.

Table S4. Quantification of immunoblots shown in Fig. 1 c

Treatment	Relative p-Ser-PKC/Coro1a
Nonstimulated	1.00
PMA/ionomycin	18.39
DNP-HSA 2 min	11.30
DNP-HSA 5 min	6.80
DNP-HSA 10 min	3.08
DNP-HSA 20 min	2.80

Densitometric quantification of the immunoblots shown in Fig. 1 c. The intensities of the phospho-Ser-PKC–specific bands were normalized to the Coro1a loading control. Values are reported in arbitrary units.

Table S5. Quantification of immunoblots shown in Fig. 1 d

Treatment	Relative p-Coro1b/Coro1b
Nonstimulated	1.00
PMA/ionomycin	6.91
DNP-HSA 2 min	6.75
DNP-HSA 5 min	5.80
DNP-HSA 10 min	5.22
DNP-HSA 20 min	5.72
DNP-HSA 40 min	4.34

Densitometric quantification of the immunoblots shown in Fig. 1 d. The intensities of the phospho-Ser2-Coro1b–specific bands were normalized to the Coro1b loading control. Values are reported in arbitrary units.

Table S6. Quantification of immunoblots shown in Fig. 1 f

Genotype	Coro1a/actin	Coro1b/actin
WT	1.14	0.94
C1a.KO	0.00	1.05
C1b.KO	1.26	0.00
DKO	0.00	0.00

Densitometric quantification of the immunoblots shown in Fig. 1 f. The actin loading control was utilized to normalize values. Values are reported in arbitrary units.

Table S7. Quantification of immunoblots shown in Fig. 2 g

Genotype	Time of stimulation	Relative p-Erk/Erk	Relative p-p38/p38
	min		
WT	0	1.00	1.00
WT	5	62.33	7.00
WT	20	52.53	3.56
C1a.KO	0	1.24	1.31
C1a.KO	5	58.08	7.31
C1a.KO	20	44.89	3.17
C1b.KO	0	0.41	1.55
C1b.KO	5	61.64	5.13
C1b.KO	20	54.79	3.58
DKO	0	1.29	1.07
DKO	5	64.42	6.57
DKO	20	52.53	1.62

Densitometric quantification of immunoblots shown in Fig. 2 g. The intensities of the phospho-specific bands were normalized to the indicated loading controls. Values are reported in arbitrary units.

Table S8. Quantification of immunoblots shown in Fig. 4 c

Treatment	Ratio soluble/pellet		
	Coro1a	Coro1b	p-Coro1b
Fig. 4 c, left			
Nonstimulated	0.40	0.44	0.83
PMA/ionomycin	0.79	1.85	14.68
Latrunculin B	3.74	1.20	1.38
Fig. 4 c, right			
Nonstimulated	0.36	0.54	1.21
DNP-HSA 2 min	0.65	2.12	7.98
DNP-HSA 5 min	0.65	2.23	8.82
DNP-HSA 20 min	0.31	0.48	1.93
DNP-HSA 60 min	0.37	0.48	1.31

Densitometric quantification of the immunoblots shown in Fig. 4 c. The ratio of band intensities in the soluble to the insoluble pellet fraction is shown. Values are reported in arbitrary units.

Table S9. Quantification of the immunoblot shown in Fig. 5 b

Analysis	Expression construct				
	Coro1a FL	S2A	S2D	R29E	S2D-R29E
Ratio soluble/pellet	0.32	0.10	1.81	5.36	3.56

Densitometric quantification of the immunoblot shown in Fig. 5 b. The ratio of band intensities in the soluble to the insoluble pellet fraction is shown. Values are reported in arbitrary units.

REFERENCES

Orinska, Z., N. Föger, M. Huber, J. Marschall, F. Mirghomizadeh, X. Du, M. Scheller, P. Rosenstiel, T. Goldmann, A. Bollinger, et al. 2010. I787 provides signals for c-Kit receptor internalization and functionality that control mast cell survival and development. *Blood*. 116:2665–2675. doi:10.1182/blood-2009-06-228460

Parravicini, V., M. Gadina, M. Kovarova, S. Odom, C. Gonzalez-Espinosa, Y. Furumoto, S. Saitoh, L.E. Samelson, J.J. O'Shea, and J. Rivera. 2002. Fyn kinase initiates complementary signals required for IgE-dependent mast cell degranulation. *Nat. Immunol*. 3:741–748.